Biofabrication

International Society for Biofabrication

PAPER

One-step delivery of a functional multi-layered cell sheet using a thermally expandable hydrogel with controlled presentation of cell adhesive proteins

Biofabrication

PAPER

One-step delivery of a functional multi-layered cell sheet using a thermally expandable hydrogel with controlled presentation of cell adhesive proteins

RECEIVED
18 April 2017

REVISED
11 November 2017

ACCEPTED FOR PUBLICATION
27 November 2017

PUBLISHED
10 January 2018

Yu Bin Lee[1,2], Joong-yup Lee[1,2], Hayeon Byun[1,2], Taufiq Ahmad[1,2], Mitsuru Akashi[3], Michiya Matsusaki[3,4] and Heungsoo Shin[1,2,4]

[1] Department of Bioengineering, Hanyang University, 222 Wangsimri-ro, Seongdong-gu, Seoul 04763, Republic of Korea
[2] BK21 Plus Future Biopharmaceutical Human Resources Training and Research Team, Hanyang University, 222 Wangsimri-ro, Seongdong-gu, Seoul 04763, Republic of Korea
[3] Department of Applied Chemistry, Graduate School of Engineering, Osaka University, 2-1 Yamada-oka, Suita 565-0871, Japan
[4] Authors to whom any correspondence should be addressed.

E-mail: hshin@hanyang.ac.kr

Keywords: 3D multi-layered cell sheet formation, layer-by-layer coating, scaffold-free tissue harvest, thermally expandable hydrogel, surface modification

Supplementary material for this article is available online

Abstract

In this study, we developed a new system enabling rapid delivery of a multi-layered cell sheet by combining layer-by-layer (LBL) coating of a cell membrane and surface engineered thermally expandable hydrogel. Human dermal fibroblasts were LBL-coated with fibronectin (FN) and gelatin to form a multi-layered cell sheet in a single seeding step via spontaneous 3D cell–cell interactions. FN was covalently immobilized onto the surface of a Tetronic®—based hydrogel at two different concentrations (1 and 5 μg ml^{-1}) for stable adhesion of the multi-layered cell sheet, followed by polydopamine coating. In both conditions, a multi-layered cell sheet was stably formed. Then, the cell sheet on the hydrogel modified with 1 μg ml^{-1} FN rapidly detached (>90% efficiency) in response to the expansion of the hydrogel when temperature changed from 37 °C to 4 °C, while the other group had a reduced detachment due to excessive cell–hydrogel interaction. The multi-layered cell sheet was evident in cell–extracellular matrix and cell–cell junction formation, and bFGF was continuously secreted over 7 days of *in vitro* culture. The multi-layered transplanted to the mouse subcutaneous tissue also exhibited evidence of vascular ingrowth, which collectively suggest that the delivery system maintaining cellular functions is applicable for regenerative medicine.

1. Introduction

Cell sheet engineering using a substrate grafted with poly(N-isopropylacrylamide) (NIPAAm) brushes has received a great deal of attention in regenerative medicine due to its ability to harvest and deliver cell monolayers for tissue regeneration without the need for implantation of foreign materials [1–3]. Upon transplantation, cell–cell and cell–extracellular matrix (ECM) interactions within the cell sheet are effectively maintained for improved functional recovery of many types of damaged tissues including cornea, heart, liver, and esophagus [4–7]. Moreover, this technique has been modified to assemble three-dimensional (3D) multi-layered constructs to mimic the complex structure of natural tissues. For example, multi-layered vascularized connective and myocardiac tissues have been developed from human aortic endothelial cells (HAEC), cardiomyocytes, and induced pluripotent stem cells [8, 9]. Multi-layered cell sheets have been mostly accomplished via layer-by-layer (LBL) stacking of an individual cell sheet using forceps or a gelatin gel plunger [10–13]. However, these processes lead to folding or shrinking of the cell sheet due to its mechanical weakness, and often require a relatively long and labor-intensive process of multi-layered cell sheet formation, which limits its use in practical applications.

Alternatively, spontaneous formation of a multi-layered cell sheet by LBL coating of cell adhesive

molecules on a cell membrane has been reported by our colleagues. Fibronectin (FN), gelatin (G), heparin, and other synthetic polymers have been repeatedly coated onto cell surfaces via electrostatic interactions to form a nano-scaled thin layer, enabling fabrication of a 3D multi-layered cell sheet [14, 15]. This *in situ* multi-layered cell sheet formation technique has been mostly utilized as an *in vitro* 3D tissue model for biological assays or drug screening. For example, 3D engineered tissue composed of human dermal fibroblasts and human umbilical vein endothelial cells was achieved to mimic the vascularization process [16]. An engineered 3D artery model was also prepared by assembling human aortic smooth muscle cells and HAEC mediated by LBL coating for simulation of nitric oxide (NO) diffusion in the artery wall [17]. However, direct transplantation of a multi-layered cell sheet from a surface has rarely been studied due to lack of an appropriate surface with the ability to support stable 3D tissue formation, which can then be readily harvested and delivered in a physiological environment. A surface modified with disulfide-cross-linked poly(γ-glutamic acid) (γ-PGA-SS) allowed for transplantation of a multi-layered cell sheet following enzymatic degradation; however, the relatively long processing time (>1 h) emphasized the need for an alternative delivery system [18].

We have developed a cell sheet delivery platform based on thermally expandable hydrogels synthesized from thermosensitive Tetronic® polymers, subsequently functionalized on the surface of hydrogels to allow controlled cell adhesion [19, 20]. In our previous studies, we demonstrated that the balance between cell attachment and thermal expansion is critical for successful formation of a cell sheet and its detachment for applications; either too weak or too strong binding of cells on the surface of the hydrogel resulted in immature cell adhesion or limited cell sheet separation, respectively [20, 21]. Stable formation of a multi-layered cell sheet on the hydrogel might be more challenging since it would generate a strong contractile force, which can result in poor adhesion of multiple layers on the hydrogel [22]. Thus, the surface of the hydrogel should be modified with cell binding molecules that are sufficiently strong to support the stable formation of a multiple-layered cell sheet while allowing rapid detachment in response to a temperature change.

Given these considerations, we modified a hydrogel surface with various concentrations of fibronectin mediated by a bio-inspired polydopamine (PD) coating process. It has been reported that secondary ligation of proteins is readily formed on PD either by protein adsorption or covalent reaction [23–25]. The objectives of the current study were to investigate the effect of fibronectin concentration (1–5 μg ml^{-1}) for hydrogel modification on the stable formation of a multi-layered cell sheet of fibroblasts prepared by LBL coating and its detachment with temperature change in order to assess the effect of cell seeding density on the number of layers of harvested cell sheets and to analyze the effect of a transplanted multi-layered cell sheet made from fibroblasts on *in vivo* engraftment and pro-angiogenic potential.

2. Experimental

2.1. Materials

Tetronic® 1307 (M W 18000) was obtained from BASF (Ludwigshafen, Germany). p-Nitrophenylchloroformate (PNC), tyramine, horseradish peroxidase (HRP), hydrogen peroxide (H_2O_2), dopamine hydrochloride, hematoxylin, gelatin, anti-mouse and anti-rabbit IgG biotin conjugates, Transwell® membranes, and other unspecified chemicals were purchased from Sigma Aldrich (St. Louis, MO, USA). Goat anti-mouse Alexa Fluor 546-conjugated IgG (A11003) was purchased from Invitrogen (Carlsbad, CA, USA). Tris-HCl was purchased from Shelton Scientific, Inc. (Peosta, IA, USA). Human dermal fibroblasts (HDFBs), high-glucose Dulbecco's modified Eagle's medium (HG-DMEM), trypsin/EDTA, and penicillin-streptomycin were obtained from Gibco BRL (Carlsbad, CA, USA). Fetal bovine serum (FBS) was purchased from Wisent (St. Bruno, QC, Canada). Human plasma fibronectin (FN) and mouse anti-fibronectin were obtained from BD Biosciences (Franklin Parks, NJ, USA). The human basic fibroblast growth factor (bFGF) ELISA kit was purchased from Peprotech (Rocky Hill, NJ, USA). The water-soluble tetrazolium salt (WST) assay kit (EZ-Cytox) was obtained from DoGen (Seoul, Korea). The Quant-iT™ PicoGreen® dsDNA assay kit, rhodamine-phalloidin, Vybrant™ DiD (red) cell-labeling solution, and live/dead® viability/cytotoxicity kit were purchased from Life Technologies Corp. (Grand Island, NY, USA). FITC-conjugated streptavidin was purchased from eBioscience (San Diego, CA, USA). Mounting medium containing 4′,6-diamidino-2-phenylindole (DAPI) was obtained from Vectashield® (Burlingame, CA, USA). Rabbit anti-collagen IV (Col IV), mouse anti-smooth muscle alpha actin (SMA), and mouse anti-CD31 antibodies were purchased from Abcam (Cambridge, MA, USA). Mouse anti-connexin 43 (Cx43) was obtained from Cell Signaling Technology Inc. (Danvers, MA, USA). Eosin was purchased from BBC Biochemical (Mt. Vernon, WA, USA).

2.2. Multi-layered cell sheet formation via LBL coating of ECM molecules

HDFBs were cultured in growth medium (10% FBS, 1% PS in HG-DMEM). Cell culture was conducted under standard conditions (95% humidity, 5% CO_2, 37 °C) on tissue culture plates (TCPs). The medium was changed every 2 days. Cells were detached from TCPs using 0.05% of trypsin/EDTA for passage and

other experiments. Detached cells were coated with FN and gelatin (G) (FN/G LBL coating) as previously described [16]. Briefly, cells were suspended in 40 μg ml^{-1} of FN solution in 10 mM Tris-HCl buffer (pH 7.0) and rotated for 1 min at 30 rpm. For FN coating, the cell suspension was centrifuged for 1 min at 2000 rpm. The cell pellet was then suspended in 10 mM Tris-HCl buffer (pH 7.0), rotated for 1 min at 30 rpm, and centrifuged for 1 min at 2000 rpm (washing step). The cell pellet was then suspended in 40 μg ml^{-1} of G solution in 10 mM Tris-HCl buffer (pH 7.0) and rotated for 1 min at 30 rpm. For G coating, the cell suspension was centrifuged for 1 min at 2000 rpm. After repeating these steps 3 times, the cells were suspended in pre-warmed media. LBL-coated HDFBs were then cultured on Transwell® membranes (Sigma Aldrich), fixed with 4% paraformaldehyde for 2 h, and embedded in paraffin blocks. After sectioning, the samples were stained with hematoxylin and eosin (H&E) and observed under an optical microscope (Nikon 2000, Japan). To determine the thickness and structure of the multi-layered cell sheet, we examined four samples per group and measured the thickness at three different points (left, center, right) in each sample.

2.3. Surface modification and characterization of the hydrogels

Hydrogels were prepared using a previously described method [26]. In brief, hydroxyl groups at the ends of the 4 arms of Tetronic® were converted to *p*-nitrophenylchloroformate (PNC) groups. The Tetronic®-PNC was then reacted with tyramine to form Tetronic®-tyramine (Tet-TA). A 12% Tet-TA solution dissolved in DW was separately mixed with 0.1 wt% H_2O_2 and 0.0025 mg ml^{-1} HRP, and the two solutions were mixed at a 1:1 volume ratio. Hydrogels after the crosslinking were then prepared in circular shape (diameter = 8 mm, thickness = 0.5 mm).

For PD coating, the hydrogels were immersed in 2 mg ml^{-1} of dopamine solution in 10 mM Tris-HCl buffer (pH 8.5) for 30 min at 37 °C. Then, the hydrogels were moved to 1 ml of 10 mM Tris-HCl buffer (pH 7) and incubated at 37 °C for 12 h. For FN adsorption, the hydrogels were immersed in FN solution (20 μg ml^{-1} for x-ray photoelectron spectroscopy (XPS) analysis, 1 and 5 μg ml^{-1} for the translocation test) in 10 mM Tris-HCl buffer (pH 7.0) for 2 h at 37 °C. Samples were divided into different preparation process groups of only PD coating (PD), immersion in FN solution (FN), and FN coating after PD coating (PD+FN). The surfaces of the hydrogels were observed with a phase contrast microscope (magnification = 100×). Changes in the chemical bonds of the hydrogel surface based on PD and FN reactions were analyzed with XPS (Theta Probe Base System, Thermo Fisher Scientific, Waltham, MA, USA).

2.4. Translocation of the multi-layered cell sheet through the thermally expandable hydrogel

We fabricated the multi-layered cell sheet by seeding cells at different concentrations of 500, 1000, and 1500 K (K = $\times 10^3$ cells cm^{-2}) and cultured the cells on the surface modified hydrogel for 24 h. The multi-layered cell sheet was observed by a phase contrast microscope (magnification = 100×). For the *in vitro* target substrate, glass coverslips were coated with FN (20 μg ml^{-1}, 2 h). For translocation, the cultured multi-layered cell sheet was then placed onto the target by inverting the hydrogel. The hydrogel was expanded by reducing the temperature to 4 °C for 10 min, and the multi-layered cell sheet was applied to the target by removing the expanded hydrogel. To assess the translocation efficiency, the translocated multi-layered cell sheets were lysed with RIPA lysis buffer (0.1% SDS, 150 mM Tris, 1% sodium deoxycholate, 1% Triton X-100, 150 mM NaCl, pH 7.2) and incubated with the PicoGreen dsDNA Assay Kit. We then divided the average of the calibrated values on targets with the values on the hydrogels to calculate the translocation efficiency. To estimate cell viability, we used the live/dead viability/cytotoxicity kit. Live/dead assay result was visualized by confocal microscope (CKX41, Olympus). 3D reconstruction was processed by Z-stacking of 30 images obtained by taking 3 μm distances. We incubated cells with the live/dead assay solution (ethidium homodimer (0.02%) and calcein-AM (0.01%) diluted in PBS) for 10 min at 37 °C, and the stained cells were observed with a fluorescent microscope (TE 2000, Nikon, Japan).

To observe the thickness and ECM and cell junction proteins, we prepared a PTFE membrane and coated it with PD (2 mg ml^{-1} in 10 mM Tris-HCl buffer, pH 8.5, 37 °C, 1 h) and FN (20 μg ml^{-1}, 37 °C, 2 h). After translocation on the PTFE membrane, the multi-layered cell sheets were embedded in paraffin, then the samples were sectioned at a thickness of 5 μm. H&E staining was conducted for thickness measurements using a previously described process. The sectioned multi-layered cell sheets were stained for Col IV, FN and Cx43. The samples were incubated with blocking solution (5% FBS) and then with primary antibodies for 1 h (1:100 dilution in 5% FBS), followed by staining with an anti-IgG biotin-conjugated secondary antibody (1:100 dilution in 5% FBS) and FITC-conjugated streptavidin (1:100 dilution in 5% FBS). The stained multi-layered cell sheets were counterstained with DAPI, mounted, and observed with a fluorescent microscope.

The secretion of bFGF from the multi-layered cell sheet formed by the 1000 K cell concentration and translocated to the FN-coated TCP was quantified by ELISA. We blocked migration of the cells by laying the PDMS in a ring-shape (outer diameter = 15 mm, inner diameter = 8 mm). The multi-layered cell sheet was cultured for 7 days. We collected the culture medium each day, and the culture medium was used as an

ELISA sample ($n = 4$). We performed the ELISA based on the provided protocol.

2.5. Transplantation of the multi-layered cell sheet to a subcutaneous mouse model

Seven-week-old female Balb/C mice were maintained based on the instructions and guidelines of the Institutional Animal Care and Use Committee (IACUC) of Hanyang University (HY-IACUC-15-0005). To anesthetize the mice, approximately 100–150 μl of anesthesia solution (0.9:0.1:4 Zoletil, Rompun, and Saline, respectively) was injected in the peritoneal cavity of each mouse. The dorsal area of the mouse was shaved and wiped with 70% EtOH for sterilization. A straight line incision of 3 cm was made on the dorsum of the mouse, and the skin was opened and held for translocation of the multi-layered cell sheet. The hydrogel carrying the multi-layered cell sheet was held under the subcutaneous area and treated with pre-chilled normal saline (4 °C) for 15 min. As the hydrogel expanded, the multi-layered cell sheet of 1500 K was transferred to the subcutaneous tissue. To examine the engraftment of the multi-layer cell sheet *in vivo*, we transferred a pre-labeled multi-layer cell sheet. HDFBs were incubated in culture medium containing diluted Vybrant™ DiD (red) cell-labeling solution in a 1:100 ratio for 1 h. The cells were sequentially trypsinized and processed for *in vivo* transplantation of 1500 K multi-layer. We observed mouse with the labeled samples for 7 days using the Image Station (4000 MM, Eastman Kodak Company, Rochester, NY, USA). The tissue area transferred with the multi-layer was retrieved after 14 days and fixed in 10% formalin solution. The fixed tissues were then processed and embedded in a paraffin mold. The paraffin-embedded tissue was sectioned into 5 μm thick tissue sections using a rotary microtome. For histological analysis, the sections were stained with H&E as described previously. We performed immunofluorescence staining for the angiogenic markers SMA and CD31 using the previously described process.

2.6. Statistical analysis

All quantitative results are indicated as the mean ± standard deviation. The statistical significance was assessed via Student's t-test and analysis of variance ANOVA, with post comparison via Tukey's HSD test ($p < 0.05$).

3. Results and discussion

The overall scheme of (1) LBL coating mediated multi-layered cell sheet formation on a thermally expandable hydrogel and (2) its ready-to-go translocation in response to temperature change is illustrated in figure 1. We hypothesized that the multi-layered cell sheet would generate a strong contractile force and the controlled presence of FN on the surface would provide an appropriate platform to harvest a multi-layered cell sheet upon temperature change.

3.1. Multi-layered cell sheet formation of HDFBs by LBL coating

The LBL coating on the surface of HDFBs was visualized using fluorescently labeled gelatin-FITC and FN-rhodamine (figure 2(a)). On the merged image of green and red fluorescent signals and phase contrast image, the green and red signals overlapped and were located on cells. The effect of the LBL coating on viability and proliferation was then assessed. Trypan blue staining showed that the HDFBs with LBL coating exhibited a viability of 90.4 ± 1.8% (figure 2(b)). The proliferation rate of HDFBs without modification was 1.8 ± 0.0 and 2.7 ± 0.0 at 2 and 3 days of culture, respectively, which was significantly increased to 2.0 ± 0.0 and 3.2 ± 0.0 for the HDFBs with LBL coating (figure 2(c)). LBL coating generally refers to a thin film coating technique using materials with opposite charges [27]. However, FN and G both have a negative charge at pH 7.0 [28]. Because of this, FN/G LBL coating on the cell surface is achieved by FN-binding domain interaction [15]. In previous studies, LBL coating of FN and G on L929 mouse fibroblasts showed overlapping signals with fluorescent dyes conjugated to the molecules, and the cells showed proliferation activity over 72 h of culture and maintained a viability over 80% [16, 29, 30]. Considering the previous results, LBL coating on HDFBs was also successfully conducted without adverse effects.

The effect of the LBL coating on a multi-layered cell sheet was then investigated by seeding different concentrations of cells after LBL coating. The group without LBL coating showed a monolayer structure at a seeding density of 500 K, however, failed to form a stable multi-layered cell sheet as the seeding density increased to 1500 K. In contrast, a tightly organized multi-layered cell sheet without a fractured structure was successfully formed from the groups with LBL coating, as shown in figure 3(a). The multi-layered cell sheet presented increasing thickness as a function of seeding density; the thickness was 35.6 ± 6.7, 59.7 ± 7.0, and 78.8 ± 9.2 μm at a seeding density of 500 K, 1000 K, and 1500 K cells cm^{-2} (figure 3(b)), respectively. A previous study demonstrated that cells with LBL coating have a strongly integrated structure since the coated molecules provide a 3D binding-domain to $\alpha_5\beta_1$ integrin receptor of the cell membrane as similar to the native ECM structure [16]. The necessity of FN/G layers on 3D tissue formation have been proved from conventional cell cultures without the modification, which produced only monolayer despite of high cell number and long-term culture. Insufficient cell–cell interactions probably due to the absence of an ECM layer without LBL coating might result in a more scattered and heterogeneous cell

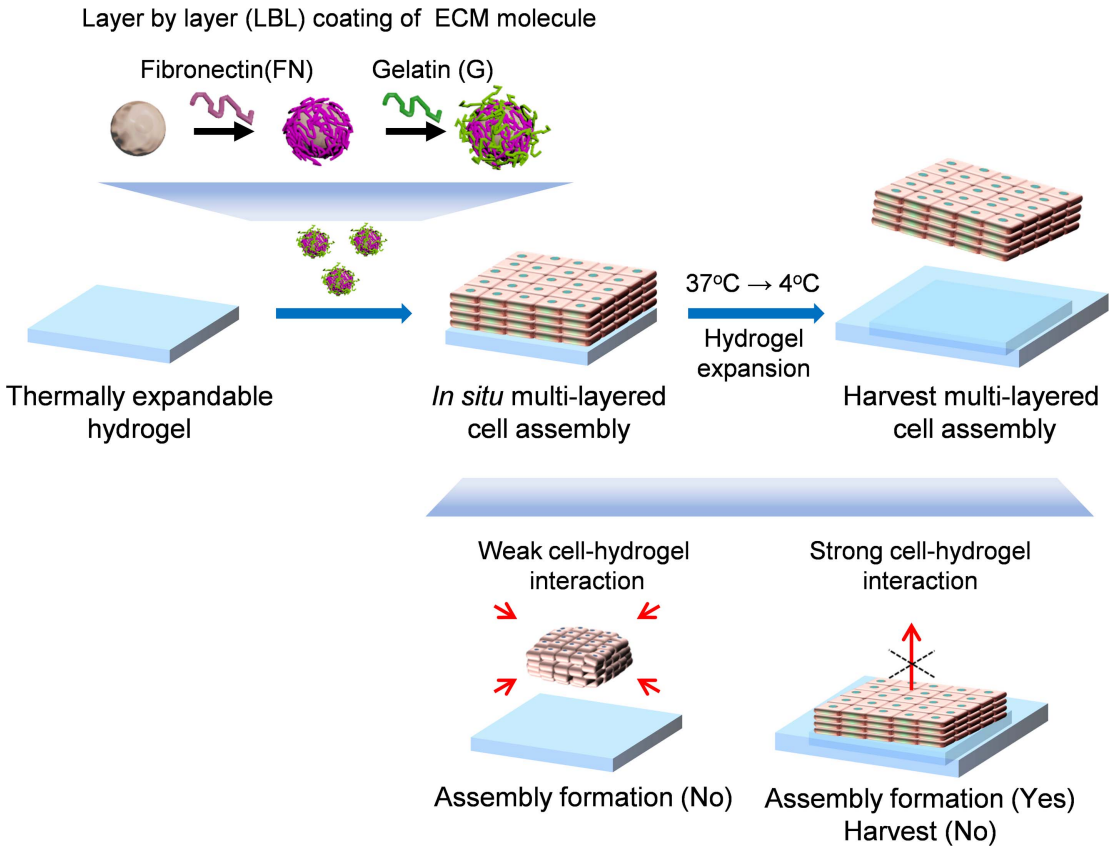

Figure 1. Schematic illustration of (1) LBL coating on cells and (2) construction of the multi-layered cell sheet on the thermally expandable hydrogel and its harvest by temperature change. We hypothesized that a weak cell–hydrogel interaction cannot support multi-layered cell sheet formation due to cellular contractility, whereas a strong cell–hydrogel interaction supports multi-layered cell sheet formation but is not appropriate for harvest. Control of the optimal cell–substrate interaction for both formation and harvest was attempted by surface modification of the thermally expandable hydrogel.

arrangement (left panel of figure 3(a)). The control of thickness of the multi-layered cell sheets depended on seeding density, which was also similar to a previous study using L929 mouse fibroblast cells [16]. As the number of L929 cells increased from 0.1 to 2.0 $\times$ 10^6, similar to our seeding densities of 100 and 2000 K, the thickness of the multi-layered cell sheet increased up to approximately 35 μm. Collectively, these results suggest that LBL coating is essential for *in situ* formation of a multi-layered cell sheet.

3.2. Surface modification of the hydrogels and cell adhesion

Surface chemical composition on the hydrogel was then analyzed via XPS (figures 4(a) and (b)). Hydrogels without modification (pristine), immersed in FN solution (FN), with PD coating (PD), and with FN coating following PD coating (PD+FN) were prepared. At 398 eV related to N1s, the PD group had an increased intensity compared to the FN group. The pristine hydrogel and FN groups were not significantly different, implying that FN cannot be solely adsorbed on hydrogel surface (data not shown). In contrast, an increased N1s peak in the PD group was similar to that in a previous study that coated PD on a Tet-hydrogel [31]. In addition, only the PD+FN group showed a slightly intensified peak at 164 eV related to S2p. In high-resolution analysis of carbon, intensified C–N and C–S peaks appeared only for the PD+FN group. It should be noted that C–N peak appeared to be decreased after coating of FN on a PD-coated hydrogel. These findings are similar to the previous report of an increase in nitrogen peak after PD coating, which lead to subsequent reduction after biomolecule coating. An alteration in the nitrogen signal may be due to making of PD-coated surface with biomolecules containing relatively lower percentage of nitrogen [32]. Collectively, our results suggest that successful FN coating on the Tet-hydrogel was only possible when mediated by the PD-coated layer. Cell interactivity of the hydrogel surfaces with different conditions was investigated by seeding LBL-coated HDFBs (figure 4(c)). When the cells were seeded at a density of 2 $\times$ 10^4 cells cm^{-2}, the pristine and FN groups could not support cell adhesion; however, both the PD and PD+FN groups showed stable adhesion of cells on their surfaces. Comparing the PD and PD+FN groups, the PD+FN group had enhanced cell adhesion. At a higher seeding density of 1 $\times$ 10^6 cells cm^{-2}, only the PD+FN group supported formation of a multi-layered cell sheet. Although the PD-coated surface also induced cell adhesion at a low seeding density, the

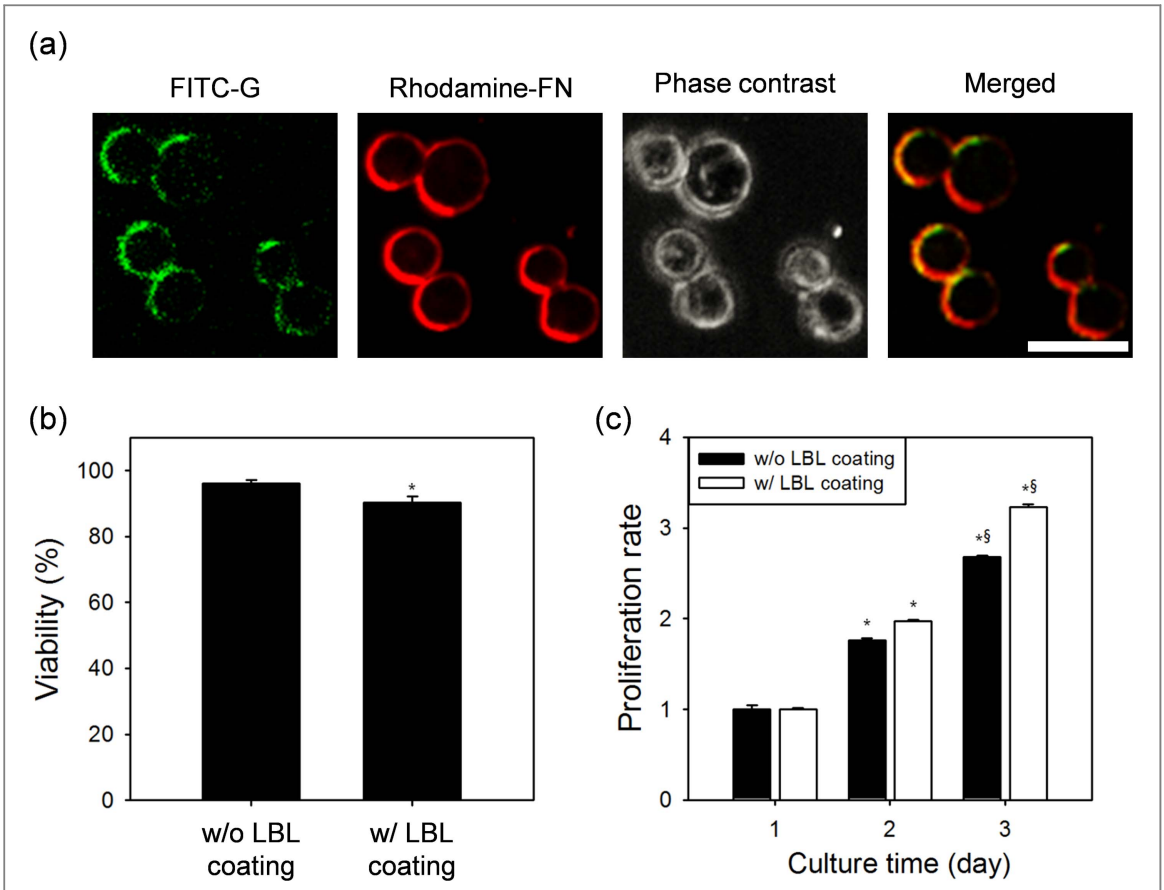

Figure 2. Effect of LBL coating on viability and proliferation of the cells. (a) Images after LBL coating of HDFBs with fluorescently-conjugated gelatin-FITC (FITC-G) and fibronectin-rhodamine (rhodamine-FN) (scale bar = 30 μm). (b) Cell viability with or without LBL coating. '*' indicates statistical significance compared to the group w/o LBL coating ($p < 0.05$). (c) Proliferation rate of cells w/o and w/LBL coating. '*' and '§' indicate statistical significance compared to the values at 1 and 2 days of culture, respectively ($p < 0.05$).

surface could not support formation of a multi-layered cell sheet, probably due to the increased contractile force [22].

Fabrication of a cell adhesive hydrogel has been achieved via both bulk and surface modification [33]. For bulk modification, cell adhesive molecules have been directly conjugated to polymer chains during the crosslinking process [34, 35]. However, inefficient presentation of the cell adhesive signal from the hydrogels and change in the mechanical properties have been regarded as technical problems [21]. Surface modification of hydrogels has been accomplished via plasma treatment, hydrolysis, and gamma ray irradiation [36]. Conjugation of cell adhesive molecules such as gelatin, FN, and RGD peptide have sequentially been conducted on functionalized hydrogels [37, 38]. However, these modification methods relied on the chemistries of the polymer composition and biomolecules, which limit their universal utility to various target surfaces. In contrast, PD coating has been employed for cell adhesive surface modification regardless of hydrogel surface chemistry. A cell-laden alginate microbead was coated with PD [39]. We also previously reported PD coating on a Tetronic®-based hydrogel, which was used for controlled cell adhesion depending on reaction parameters such as concentration of dopamine, pH, and reaction time [20, 21]. Furthermore, the PD-coated surface allows chemical immobilization of serum proteins. Our results suggest that surface immobilization of FN on the PD-coated hydrogel and thereby, increasing cell–hydrogel binding contributed stable formation of the multi-layered cell sheet.

3.3. Translocation of the multi-layered cell sheet through thermally expandable hydrogels

We then investigated the effect of FN coating concentration (1 and 5 μg ml^{-1}) on detachment of the multi-layered cell sheet. Both groups supported stable formation of the multi-layered cell sheet after seeding the LBL coated cells at a density of 1000 K. We then translocated the cell sheet from the hydrogel to glass surface by expanding the hydrogel with a change in temperature from 37 °C to 4 °C. As a result, the translocation of the multi-layered cell sheet toward the target was only observed from the group prepared with 1 μg ml^{-1} of FN while the group with 5 μg ml^{-1} of FN only exhibited scattered cells on the target surface. The delivered multi-layered cell sheet presented with an opaque white color, as indicated by the dashed circle, and had similar size and circular shape to the original hydrogel (approximate diameter = 6 mm) as shown in figure 5. We measured the amount of DNA before

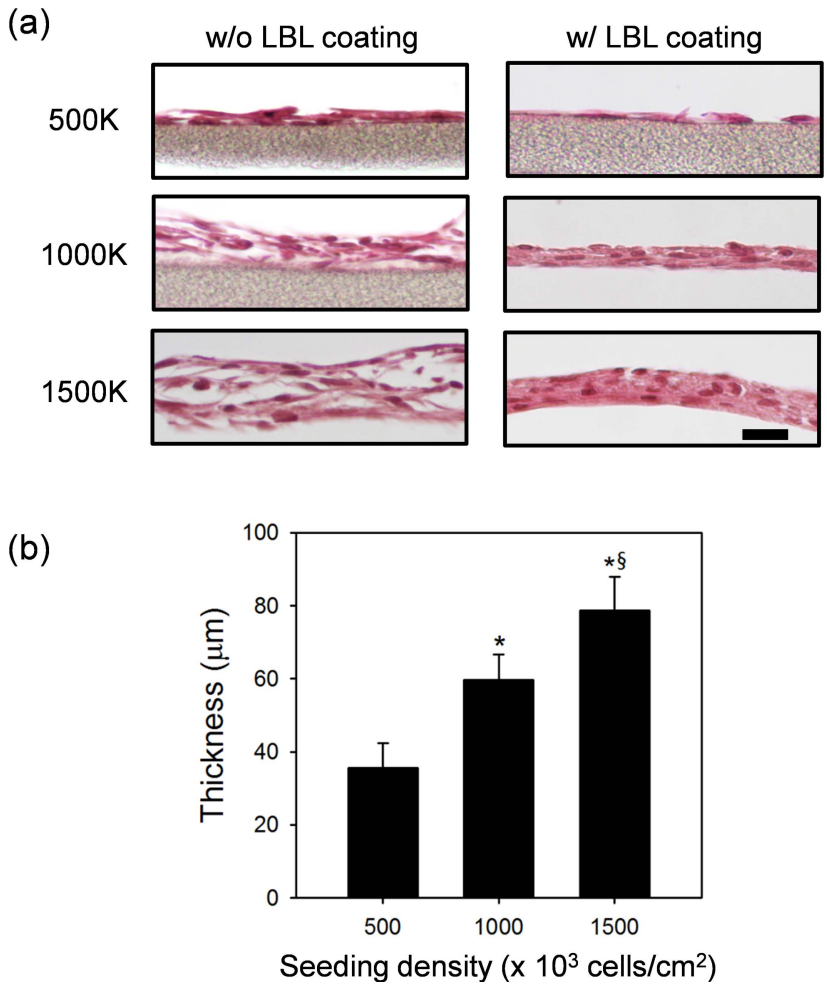

Figure 3. Analysis of the cross section and thickness estimation of multi-layered cell sheets. (a) H&E-stained multi-layered cell sheets w/o or w/LBL coating (scale bar = 100 μm). (b) The thickness of the multi-layered cell sheet depending on seeding density. '*' and '§' indicate statistical significance compared to the values of the 500 and 1000 K concentration groups, respectively ($p < 0.05$).

and after the translocation process for calculation of translocation efficiency; the 1 μg ml^{-1} FN concentration group had a high translocation efficiency of 95.8 $\pm$ 0.2%, whereas the translocation efficiency was 5.2 $\pm$ 0.5% for the 5 μg ml^{-1} FN concentration group.

Although the PD+FN-coated surface showed stable formation of the multi-layered cell sheet via enhanced cell–substrate binding, delivery of the tissue from the substrate was another challenge. The high translocation efficiency of the 1 μg ml^{-1} FN-treated group and poor delivery of the 5 μg ml^{-1} FN-treated group suggest that a moderate level of cell–hydrogel interaction is essential for the delivery. A translocation system using a PD-coated thermally expandable hydrogel previously demonstrated that excessive adhesion reduces the efficiency by impeding cell detachment [40]. For example, a translocation efficiency over 90% was achieved with an HDFB cell sheet and Tet-hydrogel with 30 min of PD coating, but 120 min of coating the hydrogel with PD presented limited translocation efficiency and viability due to impeded cell detachment [21]. In addition, the concentration of FN seems to be critical to control the adhesion strength of cells attached on the surface of biomaterials. The adhesion force of mouse fibroblasts (L929) measured by AFM also demonstrated that a higher concentration (25 μg ml^{-1}) of FN for the treated surface induces stronger cell adhesion than using a 5 μg ml^{-1} FN solution for the treated surface [41]. Collectively, modulation of cell–hydrogel binding mediated by the amount of FN was essential for stable formation of the multi-layered cell sheet by overcoming the contractility of cells and aiding delivery by allowing detachment of the multi-layered cell sheet in response to thermal expansion of the hydrogel.

3.4. Characterization of the translocated multi-layered cell sheets

The effect of seeding density on the structure of the translocated multi-layered cell sheets was then investigated. Live/dead assay images revealed that both of 1000 and 1500 K groups present favorable viability with dominant live signals (green) rarely observable dead signals (red) (figures 6(a) and supplementary data

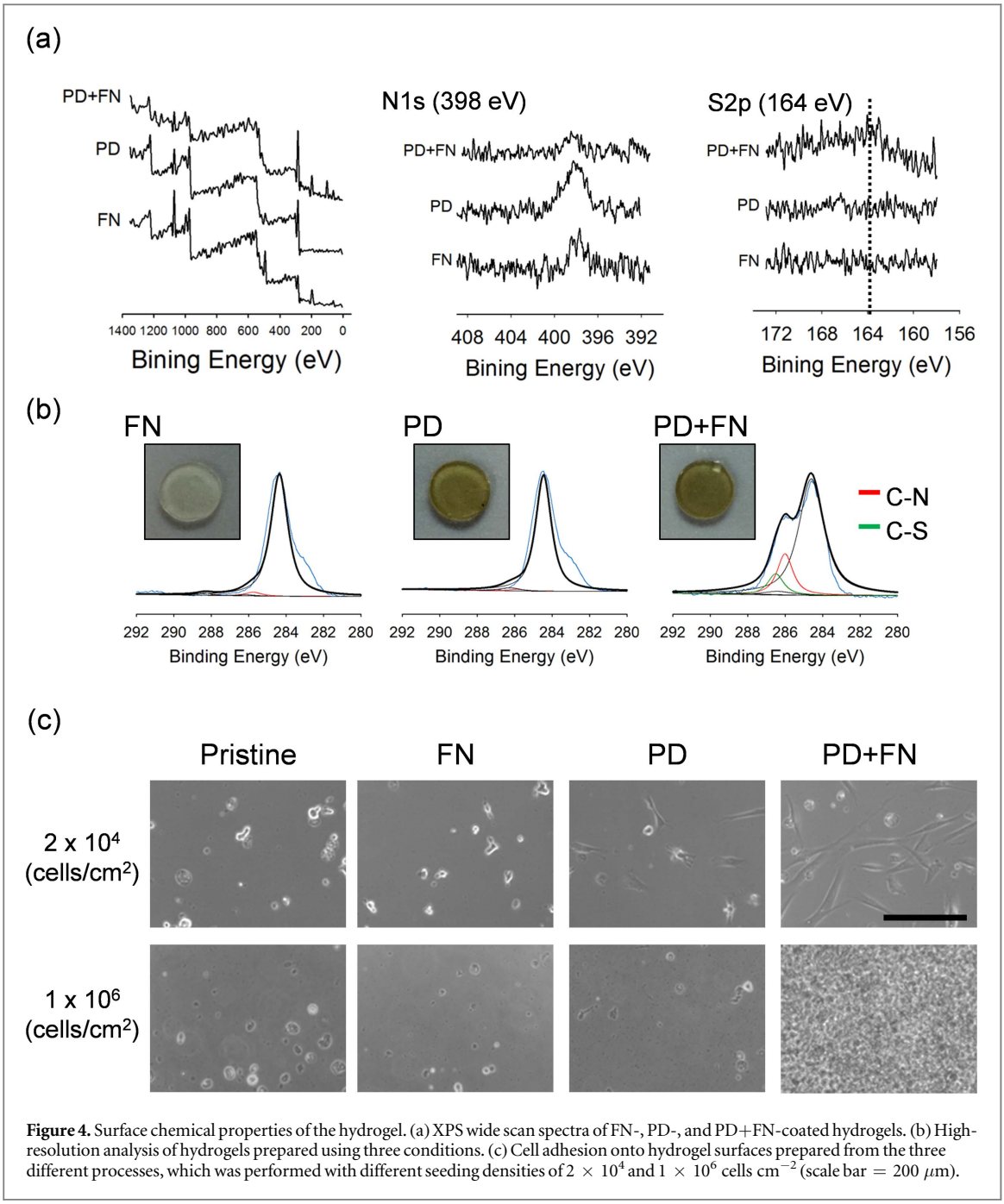

Figure 4. Surface chemical properties of the hydrogel. (a) XPS wide scan spectra of FN-, PD-, and PD+FN-coated hydrogels. (b) High-resolution analysis of hydrogels prepared using three conditions. (c) Cell adhesion onto hydrogel surfaces prepared from the three different processes, which was performed with different seeding densities of 2×10^4 and 1×10^6 cells cm^{-2} (scale bar = 200 μm).

1 is available online at stacks.iop.org/BF/10/025001/mmedia). As shown in figure 6(b), the thickness was 31.4 ± 4.9, 65.0 ± 10.1, and 150.8 ± 16.9 μm in the 500 K, 1000 K, and 1500 K concentration groups, respectively, with highly organized structures. Interesting finding was that the multi-layered cell sheet of the 1500 K group showed increased thickness after the translocation process, which may be due to enhanced cellular contractility. It was reported that a 3D collagen matrix containing pancreatic stellate cells showed an increasing contraction ratio (up to 80%) as the cell number increased from 250 to 750 K, with contractility proportional to the cell number [22]. The expression of ECM molecules and a cell junction protein was then assessed through immunofluorescence staining (1000 and 1500 K multi-layered cell sheet) (figures 6(c) and supplementary data 2(a)). Signals for collagen type IV (Col IV) and FN were distributed over the cross-section and overlapped with cell nuclei regardless of the seeding density. The cell junction protein connexin 43 (Cx43) was also well-distributed throughout the samples. The ECM not only provides physical support for structural maintenance, but also biochemical and biomechanical cues that are essential for cellular activities [42]. Cell junctions are also important for direct cell–cell and cell–ECM interactions by allowing anchoring and communication [43]. Our results demonstrated efficient retention of the microcellular environment after translocation of the multi-layered cell sheet. We also measured the secretion of bFGF from the translocated

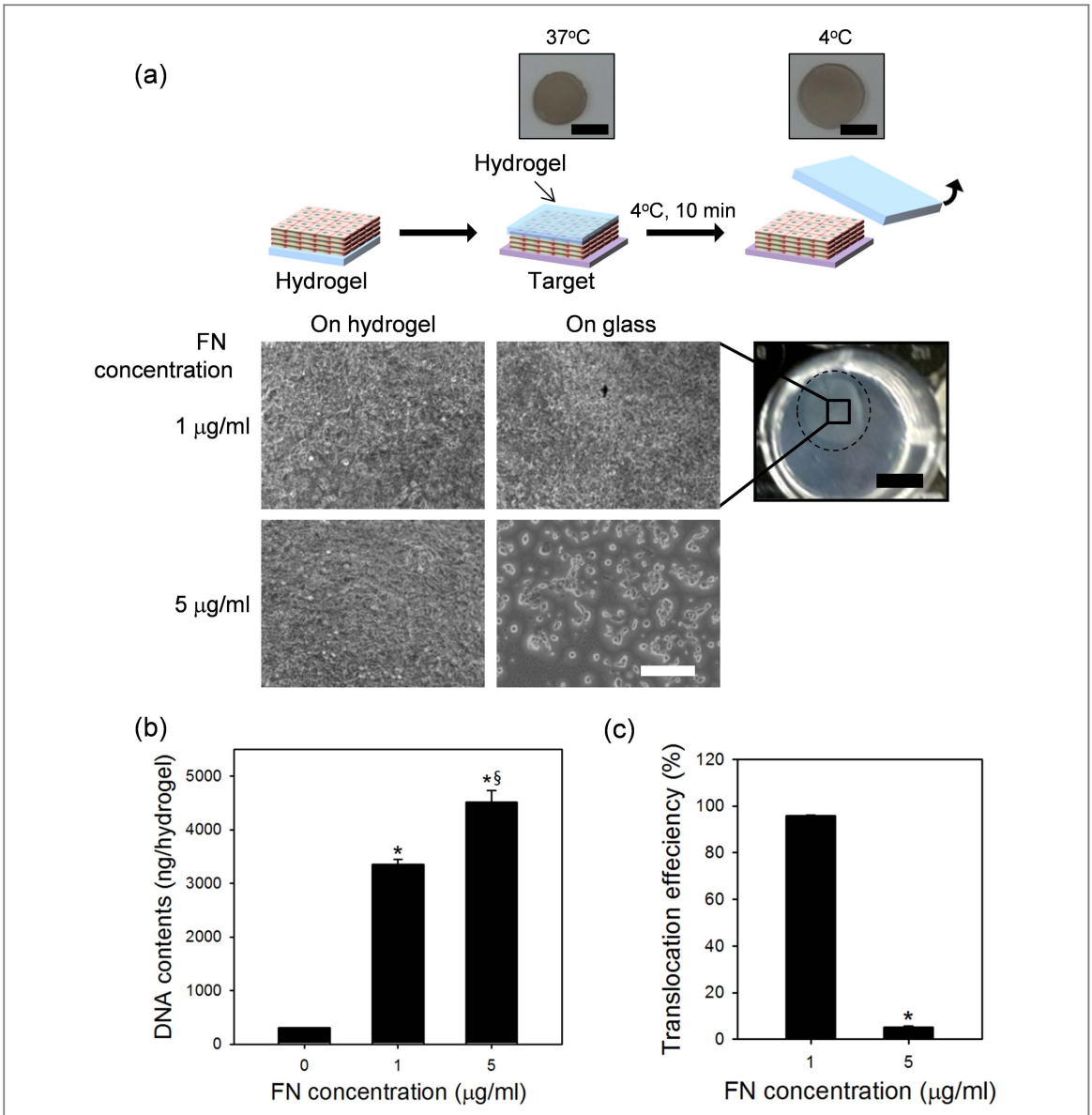

Figure 5. Translocation of the multi-layered cell sheet and efficiency of translocation. (a) Phase contrast images of cells on the hydrogel (before translocation) and on the glass substrate (after translocation) (scale bar = 200 μm). Optical images of translocated 1000 K multi-layered cell sheet (scale bar = 5 mm). (b) The DNA content of multi-layered cell sheets formed on the hydrogels treated with different concentrations of FN. '*' and '§' indicate statistical significance compared to the values of the FN-coated groups with concentrations of 0 and 1 μg ml^{-1}, respectively ($p < 0.05$). (c) Translocation efficiency depending on treated FN concentration. '*' indicates statistical significance compared to the value of the FN-coated group with a concentration of 1 μg ml^{-1} ($p < 0.05$).

1000 K group, demonstrating 0.08 ± 0.02, 0.10 ± 0.01, and 0.16 ± 0.02 ng of bFGF secretion at 1, 3, and 7 days in culture, respectively. 1500 K group exhibited increase on bFGF secretion over 0.4 ng at day 7 (supplementary data 2(b)). bFGF is one of key modulators for stimulation of proliferation and angiogenesis, and is involved in the differentiation of stem cells [44]. Collectively, these results indicate that the multi-layered cell sheet was successfully translocated from the developed thermally expandable hydrogel and proved its functionality as an engineered tissue.

Although several methods have been developed for the formation and delivery of a multi-layered cell sheet, there have been some drawbacks that limit their practical application. For example, substrates grafted with thermosensitive polymers such as NIPAAm and PEDOT require a complex process for harvesting a single layer and additional tools of cell sheet manipulators for stacking [11, 45]. A previously developed enzymatic degradable substrate with hydrophilic surface properties in response to cysteine, which cleaves disulfide bonds and exposes carboxyl groups, also demanded a long harvesting time of 1 h even though the multi-layered cell sheet formed using FN/G-coated cells was accomplished with a single seeding step [18]. However, our current method for *in situ* multi-layered cell sheet formation on the developed thermally expandable hydrogel only required 10 min for the complete delivery process and did not show any undesired changes to the structure such as shrinkage or reduced cellular functions.

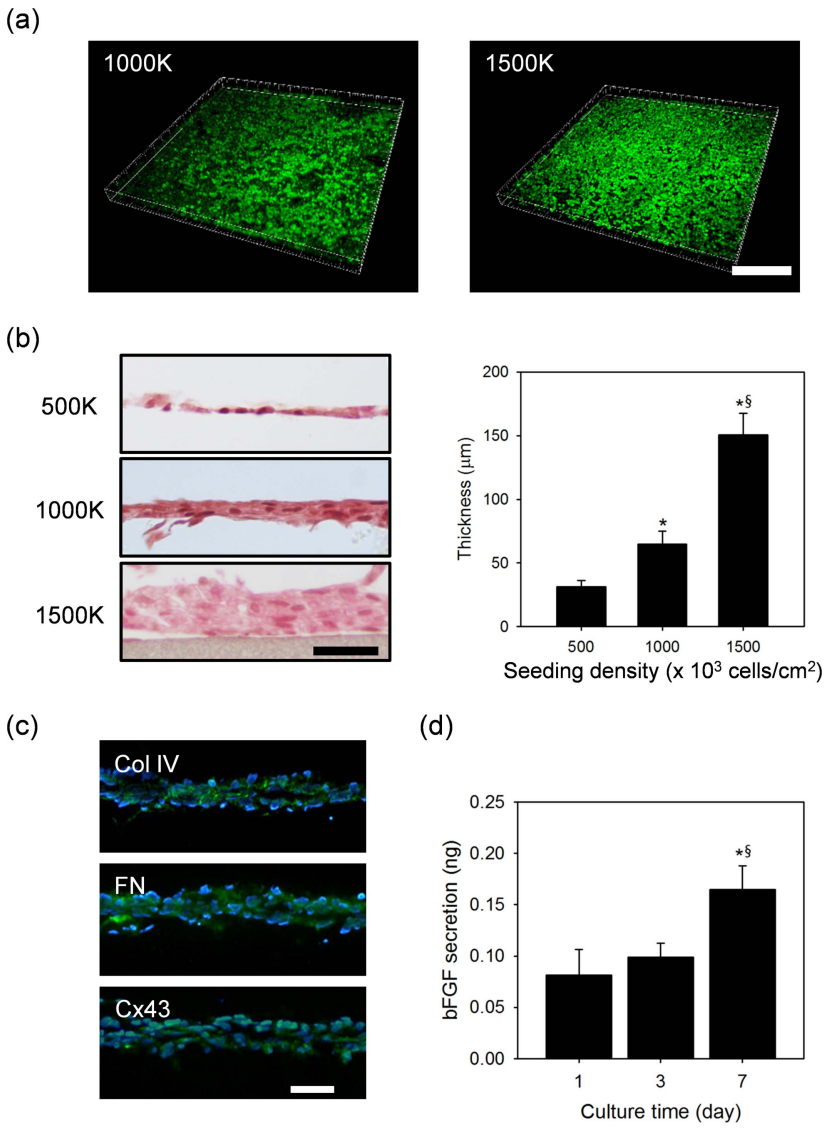

Figure 6. Structure and function of the translocated multi-layered cell sheet. (a) Live/dead assay images of translocated the multi-layered cell sheets of 1000 K and 1500 K groups (scale bar = 400 μm). (b) Cross-sections of H&E staining and thickness of the translocated multi-layered cell sheets from the hydrogel coated with 1 μg ml^{-1} of FN following PD coating (scale bar = 200 μm). '*' and '§' indicate statistical significance compared to the values of the 500 K and 1000 K concentration groups, respectively ($p < 0.05$). (c) Immunofluorescence staining of multi-layered cell sheets prepared with the 1000 K concentration, stained for ECM proteins (Col IV and FN) and a cell junction protein (Cx43) (scale bar = 100 μm). (d) bFGF secretion from the multi-layered cell sheet of the 1000 K group evaluated through ELISA. '*' and '§' indicate statistical significance compared to the values at 1 and 3 days of culture, respectively ($p < 0.05$).

3.5. Translocation and engraftment of the multi-layered cell sheet to a subcutaneous mouse model

We then assessed the feasibility of direct translocation of multi-layered cell sheet from the hydrogel to an *in vivo* target and investigated interactions of the transplanted cells with host tissue. As shown in figure 7(a), the retention of fluorescent signal over 7 days at the transplanted location confirmed the successful transplantation of multi-layered cell sheet on the subcutaneous tissue. After 14 days of transplantation, tissue samples were collected and cross-sectioned to observe the multi-layered cell sheet (figure 7(b)). Highly dense cell signals indicated by the black dashed line were observed in the region of the tissue sample with translocation, which did not exist in the control group (normal tissue). More importantly, in a high magnification image, vessel-like structures were observed within the area of dense cell signals. Immunohistochemistry confirmed that the expression of the vascular markers SMA and cluster of differentiation 31 (CD31) was observed within the area estimated as the delivered multi-layered cell sheet, but these markers were not expressed in the controls (figures 7(c), (d)). The development of vessel ingrowth may have been affected by bFGF secreted by the multi-layered cell sheet, which was observed *in vitro* experiment. SMA and CD31, which were expressed inside the translocated cell sheet, are respectively markers of arterioles and capillaries [46]. A multi-layered cell sheet composed of HDFBs and HAECs previously exhibited CD31 signals inside the

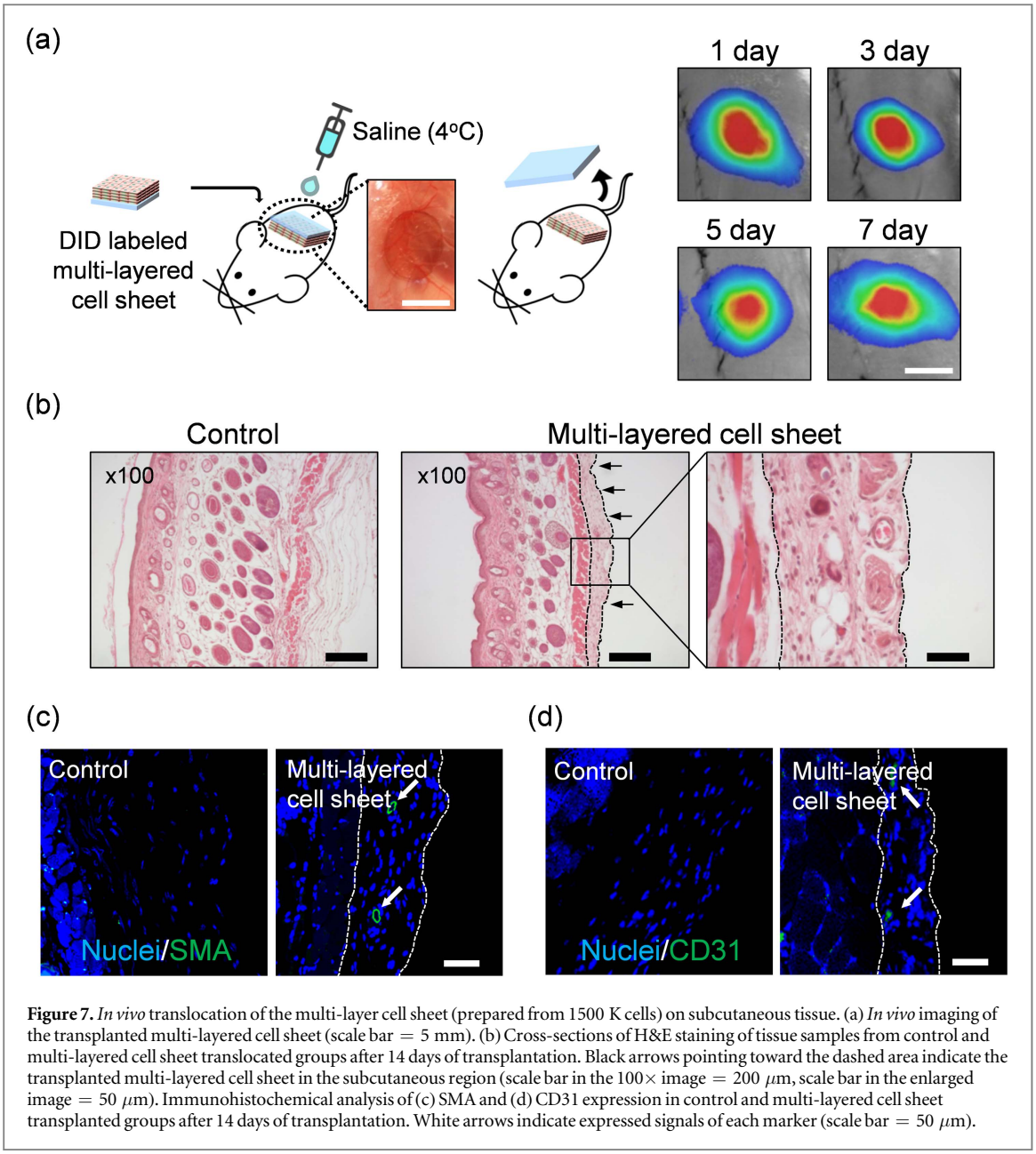

Figure 7. *In vivo* translocation of the multi-layer cell sheet (prepared from 1500 K cells) on subcutaneous tissue. (a) *In vivo* imaging of the transplanted multi-layered cell sheet (scale bar = 5 mm). (b) Cross-sections of H&E staining of tissue samples from control and multi-layered cell sheet translocated groups after 14 days of transplantation. Black arrows pointing toward the dashed area indicate the transplanted multi-layered cell sheet in the subcutaneous region (scale bar in the 100× image = 200 μm, scale bar in the enlarged image = 50 μm). Immunohistochemical analysis of (c) SMA and (d) CD31 expression in control and multi-layered cell sheet transplanted groups after 14 days of transplantation. White arrows indicate expressed signals of each marker (scale bar = 50 μm).

sheet after delivery to the subcutaneous region. A dual layer of HDFBs also secreted angiogenic factors such as hepatocyte growth factor, placenta growth factor, and matrix metalloproteinase-9 (MMP-9) [47]. Our *in vivo* results of high retention ability and vessel ingrowth demonstrated that the translocated multi-layered cell sheet interacted with the host tissue.

Multi-layered cell sheets have been used for hindlimb ischemia disease or myocardial infarction models and presented therapeutic effects through interactions with host tissue [48, 49]. They were also developed as a 3D contractile skeletal muscle tissue model or vascularized 3D tissue [50, 51]. Delivery of higher cell numbers via a multi-layered cell sheet into damaged tissue will be more effective for therapeutic applications compared to the use of a monolayer cell sheet. The multi-layered structure can increase paracrine molecule secretion and stable retention due to increased levels of ECM proteins as previously described [52–55]. Our results suggest that the developed hydrogel substrate can deliver a multi-layered cell sheet onto *in vitro* and *in vivo* targets in a rapid process time within 10 min, which hold great promise in a variety of applications. Nevertheless, quantification of immobilized FN on the PD-coated surface and measurement of cell–substrate binding force and contractile force of the multi-layered cell sheet based on cell number are additionally required for complete understanding of the developed system.

4. Conclusion

In this study, we modified a thermally expandable hydrogel surface using catecholamine chemistry to develop a multi-layered cell sheet harvest system. FN/G

LBL coating was first investigated by observing signals of fluorescent dye-conjugated FN and G that overlapped with the locations of cells. The spontaneous multi-layered cell sheet was achieved only after LBL coating, and the thickness as a function of cell seeding density was assessed by H&E staining of the cross section. Immobilization of FN via PD coating was confirmed through XPS analysis by observation of peaks related to sulfur that were not present in other groups. Stabile formation of the multi-layered cell sheet was only enabled on the FN-adsorbed surface, implying an increased cell–hydrogel interaction through ligand-receptor binding. Moderate introduction of FN at a concentration of 1 μg ml^{-1} on the PD-coated surface demonstrated a high delivery efficiency over 90%, whereas an FN concentration of 5 μg ml^{-1} showed limited translocation due to excessive binding between the modified surface and multi-layered cell sheet. Multi-layered cell sheets with controlled thickness from 31.4 ± 4.9 to 150.8 ± 16.9 μm were translocated through a simple and rapid process and exhibited maintained functions such as expression of ECM and junction proteins and bFGF secretion. Delivery of the multi-layered cell sheet to the mouse subcutaneous region showed high retention ability over 14 days of culture and induced vessel ingrowth as demonstrated by IHC to reveal expression of CD31 and SMA in the engrafted multi-layered cell sheets. Collectively, these results suggest that the developed system for delivering a multi-layered cell sheet with a simple process is a promising tool for various applications in regenerative medicine.

Acknowledgments

This work was supported by a National Research Foundation of Korea (NRF) grant funded by the Korean government (MSIP) (NRF-2017K2A9A2A08000171).

ORCID iDs

Heungsoo Shin https://orcid.org/0000-0002-9036-155X

References

[1] Yamato M and Okano T 2004 Cell sheet engineering *Mater. Today* **7** 42–7
[2] Matsuura K, Utoh R, Nagase K and Okano T 2014 Cell sheet approach for tissue engineering and regenerative medicine *J. Control. Release* **190** 228–39
[3] Guven S, Chen P, Inci F, Tasoglu S, Erkmen B and Demirci U 2015 Multiscale assembly for tissue engineering and regenerative medicine *Trends Biotechnol.* **33** 269–79
[4] Nishida K *et al* 2004 Corneal reconstruction with tissue-engineered cell sheets composed of autologous oral mucosal epithelium *New Engl. J. Med.* **351** 1187–96
[5] Masumoto H *et al* 2014 Human iPS cell-engineered cardiac tissue sheets with cardiomyocytes and vascular cells for cardiac regeneration *Sci. Rep.* **4** 6716
[6] Nagamoto Y, Takayama K, Ohashi K, Okamoto R, Sakurai F, Tachibana M, Kawabata K and Mizuguchi H 2016 Transplantation of a human iPSC-derived hepatocyte sheet increases survival in mice with acute liver failure *J. Hepatology* **64** 1068–75
[7] Ohki T, Yamato M, Murakami D, Takagi R, Yang J, Namiki H, Okano T and Takasaki K 2006 Treatment of oesophageal ulcerations using endoscopic transplantation of tissue-engineered autologous oral mucosal epithelial cell sheets in a canine model *Gut* **55** 1704–10
[8] Sekine H, Shimizu T, Sakaguchi K, Dobashi I, Wada M, Yamato M, Kobayashi E, Umezu M and Okano T 2013 *In vitro* fabrication of functional three-dimensional tissues with perfusable blood vessels *Nat. Commun.* **4** 1399
[9] Matsuo T *et al* 2015 Efficient long-term survival of cell grafts after myocardial infarction with thick viable cardiac tissue entirely from pluripotent stem cells *Sci. Rep.* **5** 16842
[10] Ren L, Ma D, Liu B, Li J, Chen J, Yang D and Gao P 2014 Preparation of three-dimensional vascularized MSC cell sheet constructs for tissue regeneration *Biomed. Res. Int.* **2014** 301279
[11] Haraguchi Y *et al* 2012 Fabrication of functional three-dimensional tissues by stacking cell sheets *in vitro Nat. Protocols* **7** 850–8
[12] Tang Z L, Akiyama Y and Okano T 2012 Temperature-responsive polymer modified surface for cell sheet engineering *Polymers* **4** 1478–98
[13] Akimoto J, Arauchi A, Nakayama M, Kanaya R, Iwase Y, Takagi S, Yamato M and Okano T 2014 Facile cell sheet manipulation and transplantation by using *in situ* gelation method *J. Biomed. Mater. Res.* B **102** 1659–68
[14] Matsusaki M, Kadowaki K, Nakahara Y and Akashi M 2007 Fabrication of cellular multilayers with nanometer-sized extracellular matrix films *Angew. Chem., Int. Ed. Engl.* **46** 4689–92
[15] Matsusaki M 2012 Development of three-dimensional tissue models based on hierarchical cell manipulation using nanofilms *Bull. Chem. Soc. Japan* **85** 401–14
[16] Nishiguchi A, Yoshida H, Matsusaki M and Akashi M 2011 Rapid construction of three-dimensional multilayered tissues with endothelial tube networks by the cell-accumulation technique *Adv. Mater.* **23** 3506–10
[17] Matsusaki M, Amemori S, Kadowaki K and Akashi M 2011 Quantitative 3D analysis of nitric oxide diffusion in a 3D artery model using sensor particles *Angew. Chem., Int. Ed. Engl.* **50** 7557–61
[18] Nishiguchi A, Matsusaki M, Miyagawa S, Sawa Y and Akashi M 2015 Dynamic nano-interfaces enable harvesting of functional 3D-engineered tissues *Adv. Healthcare Mater.* **4** 1164–8
[19] Jun I, Lee Y B, Choi Y S, Engler A J, Park H and Shin H 2015 Transfer stamping of human mesenchymal stem cell patches using thermally expandable hydrogels with tunable cell-adhesive properties *Biomaterials* **54** 44–54
[20] Lee Y B, Shin Y M, Kim E M, Lim J, Lee J Y and Shin H 2016 Facile cell sheet harvest and translocation mediated by a thermally expandable hydrogel with controlled cell adhesion *Adv. Healthcare Mater.* **5** 2320–4
[21] Lee Y B, Shin Y M, Kim E M, Lee J-Y, Lim J, Kwon S K and Shin H 2016 Mussel adhesive protein inspired coatings on temperature-responsive hydrogels for cell sheet engineering *J. Mater. Chem.* B **4** 6012–22
[22] Robinson B K, Cortes E, Rice A J, Sarper M and Del Rio Hernandez A 2016 Quantitative analysis of 3D extracellular matrix remodelling by pancreatic stellate cells *Biol. Open* **5** 875–82
[23] Lynge M E, van der Westen R, Postma A and Stadler B 2011 Polydopamine—a nature-inspired polymer coating for biomedical science *Nanoscale* **3** 4916–28
[24] Liu Y, Ai K and Lu L 2014 Polydopamine and its derivative materials: synthesis and promising applications in energy, environmental, and biomedical fields *Chem. Rev.* **114** 5057–115

[25] Perikamana S K M, Lee J, Lee Y B, Shin Y M, Lee E J, Mikos A G and Shin H 2015 Materials from mussel-inspired chemistry for cell and tissue engineering applications *Biomacromolecules* **16** 2541–55
[26] Park K M, Shin Y M, Joung Y K, Shin H and Park K D 2010 *In situ* forming hydrogels based on tyramine conjugated 4-Arm-PPO-PEO via enzymatic oxidative reaction *Biomacromolecules* **11** 706–12
[27] Lee J S, Cho J, Lee C, Kim I, Park J, Kim Y M, Shin H, Lee J and Caruso F 2007 Layer-by-layer assembled charge-trap memory devices with adjustable electronic properties *Nat. Nanotechnol.* **2** 790–5
[28] Matsusaki M and Akashi M 2014 Control of extracellular microenvironments using polymer/protein nanofilms for the development of three-dimensional human tissue chips *Polym. J.* **46** 524–36
[29] Matsuzawa A, Matsusaki M and Akashi M 2013 Effectiveness of nanometer-sized extracellular matrix layer-by-layer assembled films for a cell membrane coating protecting cells from physical stress *Langmuir* **29** 7362–8
[30] Kadowaki K, Matsusaki M and Akashi M 2010 Control of cell surface and functions by layer-by-layer nanofilms *Langmuir* **26** 5670–8
[31] Lee Y B, Shin Y M, Lee J H, Jun I, Kang J K, Park J C and Shin H 2012 Polydopamine-mediated immobilization of multiple bioactive molecules for the development of functional vascular graft materials *Biomaterials* **33** 8343–52
[32] Pan C J, Pang L Q, Gao F, Wang Y N, Liu T, Ye W and Hou Y H 2016 Anticoagulation and endothelial cell behaviors of heparin-loaded graphene oxide coating on titanium surface *Mater. Sci. Eng.* C **63** 333–40
[33] Vladkova T G 2010 Surface engineered polymeric biomaterials with improved biocontact properties *Int. J. Polym. Sci.* **2010** 22–43
[34] Van Vlierberghe S, Dubruel P and Schacht E 2011 Biopolymer-based hydrogels as scaffolds for tissue engineering applications: a review *Biomacromolecules* **12** 1387–408
[35] Tan H P and Marra K G 2010 Injectable, biodegradable hydrogels for tissue engineering applications *Materials* **3** 1746–67
[36] Plunkett K N, Chatterjee A N, Aluru N R and Moore J S 2003 Surface-modified hydrogels for chemoselective bioconjugation *Macromolecules* **36** 8846–52
[37] Van Vlierberghe S, Vanderleyden E, Boterberg V and Dubruel P 2011 Gelatin functionalization of biomaterial surfaces: strategies for immobilization and visualization *Polymers* **3** 114–30
[38] Jacob J T, Rochefort J R, Bi J J and Gebhardt B M 2005 Corneal epithelial cell growth over tethered-protein/peptide surface-modified hydrogels *J. Biomed. Mater. Res.* B **72B** 198–205
[39] Kim B J *et al* 2014 Cytoprotective alginate/polydopamine core/shell microcapsules in microbial encapsulation *Angew. Chem., Int. Ed. Engl.* **53** 14443–6
[40] Lee Y B, Shin Y M, Kim E M, Lim J, Lee J Y and Shin H 2016 Facile cell sheet harvest and translocation mediated by a thermally expandable hydrogel with controlled cell adhesion *Adv. Healthcare Mater.* **5** 2320–24
[41] Elter P, Weihe T, Buhler S, Gimsa J and Beck U 2012 Low fibronectin concentration overcompensates for reduced initial fibroblasts adhesion to a nanoscale topography: single-cell force spectroscopy *Colloids Surf.* B **95** 82–9
[42] Frantz C, Stewart K M and Weaver V M 2010 The extracellular matrix at a glance *J. Cell Sci.* **123** 4195–200
[43] Sohl G and Willecke K 2004 Gap junctions and the connexin protein family *Cardiovasc. Res.* **62** 228–32
[44] Turner N and Grose R 2010 Fibroblast growth factor signalling: from development to cancer *Nat. Rev. Cancer* **10** 116–29
[45] Kim J D, Heo J S, Park T, Park C, Kim H O and Kim E 2015 Photothermally induced local dissociation of collagens for harvesting of cell sheets *Angew. Chem., Int. Ed. Engl.* **54** 5869–73
[46] Bak S, Ahmad T, Lee Y B, Lee J Y, Kim E M and Shin H 2016 Delivery of a cell patch of cocultured endothelial cells and smooth muscle cells using thermoresponsive hydrogels for enhanced angiogenesis *Tissue Eng.* A **22** 182–93
[47] Sasagawa T, Shimizu T, Yamato M and Okano T 2014 Expression profiles of angiogenesis-related proteins in prevascular three-dimensional tissues using cell-sheet engineering *Biomaterials* **35** 206–13
[48] Kito T *et al* 2013 iPS cell sheets created by a novel magnetite tissue engineering method for reparative angiogenesis *Sci. Rep.* **3** 1418
[49] Alshammary S, Fukushima S, Miyagawa S, Matsuda T, Nishi H, Saito A, Kamata S, Asahara T and Sawa Y 2013 Impact of cardiac stem cell sheet transplantation on myocardial infarction *Surg. Today* **43** 970–6
[50] Ito A, Yamamoto Y, Sato M, Ikeda K, Yamamoto M, Fujita H, Nagamori E, Kawabe Y and Kamihira M 2014 Induction of functional tissue-engineered skeletal muscle constructs by defined electrical stimulation *Sci. Rep.* **4** 4781
[51] Sakaguchi K, Shimizu T, Horaguchi S, Sekine H, Yamato M, Umezu M and Okano T 2013 *In vitro* engineering of vascularized tissue surrogates *Sci. Rep.* **3** 1316
[52] Rajagopalan P, Shen C J, Berthiaume F, Tilles A W, Toner M and Yarmush M L 2006 Polyelectrolyte nano-scaffolds for the design of layered cellular architectures *Tissue Eng.* **12** 1553–63
[53] Ohno M, Motojima K, Okano T and Taniguchi A 2009 Maturation of the extracellular matrix and cell adhesion molecules in layered co-cultures of HepG2 and endothelial cells *J. Biochem.* **145** 591–7
[54] Chang D, Shimizu T, Haraguchi Y, Gao S, Sakaguchi K, Umezu M, Yamato M, Liu Z and Okano T 2015 Time course of cell sheet adhesion to porcine heart tissue after transplantation *PLoS One* **10** e0137494
[55] Kainuma S *et al* 2015 Cell-sheet therapy with omentopexy promotes arteriogenesis and improves coronary circulation physiology in failing heart *Mol. Ther.* **23** 374–86